1-1-1994

Focus Optimization of a Cryogenic Collimater Using Interferometric Measurements and Optical Modeling

Joe Tansock

Alan Thurgood

Roy Esplin

Focus Optimization of a Cryogenic Collimator using Interferometric Measurements and Optical Modeling

Joe Tansock, Alan Thurgood, Roy Esplin

Space Dynamics Laboratory/Utah State University
1747 North Research Parkway, Logan, UT 84321

ABSTRACT

Space Dynamics Laboratory at Utah State University (SDL/USU) optimized the focus of an off-axis, cryogenically cooled infrared collimator for cryogenic operating temperatures. Historically, collimator focus was optimized at ambient temperatures where interactive focus adjustment and testing could be performed. The focus shift that occurred when the optics were cooled was minimized by collimator design, and the change was negligible compared to the spatial resolution of the IR sensor measuring the collimator's simulated point source. However, the focus determined at ambient temperature does not meet the image quality requirements of state-of-the-art sensors. The method used by SDL to determine optimal focus at cryogenic temperatures applies classical optical techniques to the cryogenically cooled environment. System level interferometric measurements are first made to characterize the system wavefront error. These measurements are then applied to an aberration-free optical model to evaluate system focus for a wavelength of 12 μm. The method also uses a knife edge test to refer the interferometric measurements to the aperture located near the focal point of the collimator. This paper discusses the physical test setup, outlines the optical model and analysis procedure, and presents results before and after focus optimization of a multifunction infrared calibrator.

Keywords: cryogenic, IR collimator, focus, optical model, wavefront error

1. INTRODUCTION

The nearly diffraction-limited image quality and spatial detection of state-of-the-art IR imaging sensors place stringent requirements on the image quality and focus of collimators used to simulate point sources during calibration. Historically, collimator focus was optimized at ambient temperature where interactive focus evaluation and adjustment could be performed. The shift in focus due to cooling the optics, which in turn affected the image quality, was made negligible by designing the collimator with a long focal length.

The relationship between focus shift and image quality can be evaluated to a first order by comparing the optical path difference (OPD) due to defocus against the Rayleigh criterion. The OPD due to longitudinal defocus of magnitude δ is approximated by Equation (1), derived from Smith[1] (equation 11.1),

$$OPD \approx \frac{\delta}{8\,(f/D)^2} = \frac{\delta}{8\,(F)^2} \tag{1}$$

where f = system focal length and D = exit pupil diameter. The Rayleigh criterion specifies that a peak-to-valley wavefront error of λ/4 or less would not seriously affect the image quality of a system[2] and the system performance may be approximated by the diffraction limit. Setting the OPD equal to the Rayleigh criterion, the permissible focus shift for a diffraction limited system is shown in Equation (2).

$$\delta_{max} \approx \frac{\lambda}{4} \times 8\,(f/D)^2 \tag{2}$$

0-8194-1592-8/94/$6.00

For $\lambda = 12$ μm, which was the wavelength of interest for this study, a system with a focal length of 200 inches and exit pupil diameter of 16 inches, δ_{max} is 0.148 inches, showing that image quality is sensitive to small focus shifts for even relatively long focal length systems. For systems where aberrations are significant relative to the diffraction limit, the problem of identifying the permissible focus shift from cooling the optics becomes more complicated. In general, however, a system approaching the geometric limit is more sensitive to defocus than the diffraction-limited system. Therefore, optimizing the focus of a cryogenic collimator is desirable when the collimator is used to calibrate state-of-the-art imaging IR sensors.

In addition to the variation in image quality with focus shifts, cryogenic systems also require long periods between successive tests because of the need to pump and cool the instruments. Time constraints usually prohibit successive iterations to refine the optimal focus.

SDL applied system level interferometric measurements to an aberration-free optical model to determine the optimum focus of a cryogenic multifunction infrared calibration source (MIC2). The usefulness of coupling interferometric measurements with optical design analysis was demonstrated by Willey and Patchin[3]. SDL first performed detailed interferometric image quality testing to characterize the system wavefront error. The characterized wavefront or equivalently geometric aberration was then included in an aberration-free optical model to identify best focus for the intended application. After an implemented focus refinement, image quality testing and analysis were repeated to verify the new focus. As a result, one cold cycle was required to identify optimum focus and a second to verify the optimized focus. This paper discusses the physical test setup, outlines the optical model and analysis procedure, and presents results before and after focus adjustment of MIC2.

2. CRYOGENIC COLLIMATOR

MIC2 was designed and built by SDL/USU and combines multiple source configurations into a single cryogenically cooled infrared (IR) calibrator. The concept and methodology for multiple source IR calibrators is discussed in Wyatt, et al. (1988)[4]. The optics are cooled to cryogenic temperatures with an internal liquid cryogen holding tank. In collimator mode, MIC2 provides a distant, small-area, full-entrance-aperture source through an off-axis Gregorian telescope with an effective focal length of 200 inches. A blackbody source positioned behind a pinhole located at the focal plane simulates a point source for imaging IR sensors attached to the exit port. A flat mirror mounted on a two-axis gimbal allows the source to be moved in object space. Figure 1 shows a ray trace of MIC2 configured in collimator mode.

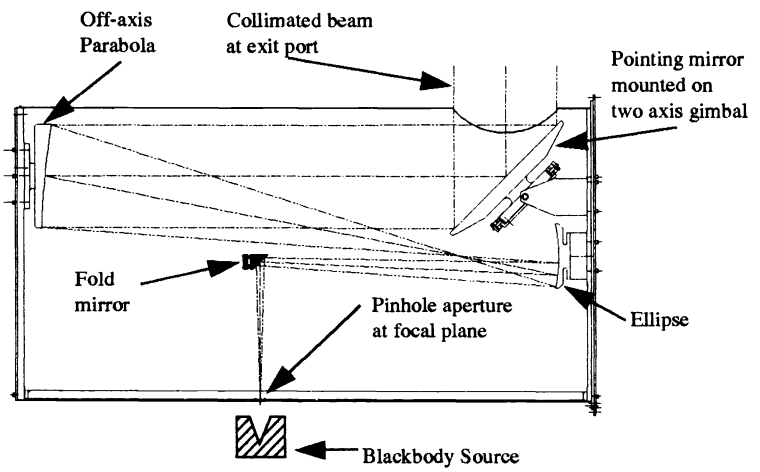

Figure 1. MIC2 ray trace for collimator configuration.

3. METHODS

3.1 Image Quality Test Setup

The first step we used to evaluate the collimator's focus was to characterize the system wavefront error by performing detailed interferometric image quality testing. This testing collected system level interferograms of the collimator's optics that were used to characterize geometric aberrations. An interferogram represents a wavefront error or optical path difference (OPD) where each fringe is a line of constant OPD and adjacent fringes differ in OPD by one wavelength of the source light.

A long unequal path interferometer (LUPI)[5] was used in a double pass configuration to measure the image quality of MIC2 at liquid helium (LHe) temperatures. The interferometer light source consisted of a HeNe laser with $\lambda = 0.6328$ μm. A double pass interferometric experiment basically consists of an interferometer that compares a reference beam of light with light that has traveled twice through the optical system being tested (test beam). The measured result is an interferogram with bright fringes where the reference beam constructively interferes with the test beam. Figure 2 shows a simple schematic of the double pass configuration.

Figure 3 shows the MIC2 image quality test setup. The LUPI was located at MIC2's entrance port where the focal point of the collimator was located. On the front of the LUPI and in the path of the test beam, an F10 diverger was used to create a focused beam that over-filled MIC2's optics. The test beam of the interferometer passed through the collimator, antechamber, and vacuum interface window. This beam then reflected off the warm optically flat mirror and returned in the reverse order to the interferometer, comprising the double pass configuration. The purpose of the 16-inch diameter, 120-inch long antechamber attached to MIC2's exit port was to limit room temperature throughput into MIC2 and to reduce the thermal gradients on the vacuum interface window located at the end of the antechamber.

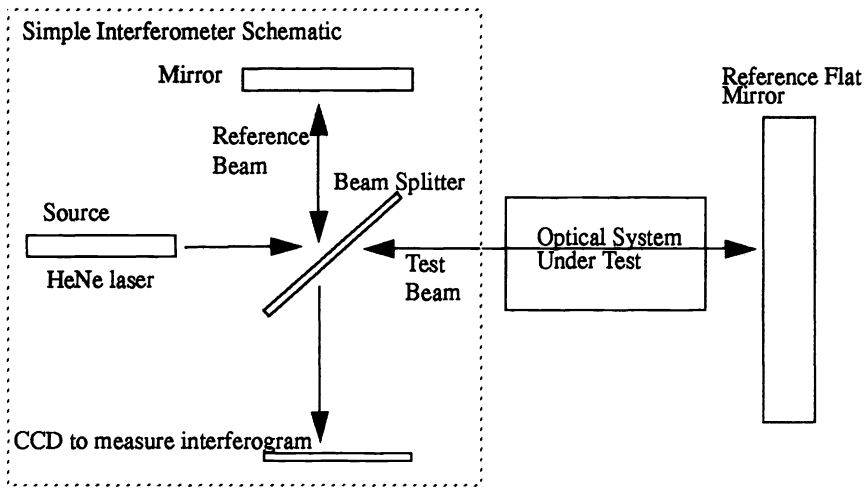

Figure 2. Simple schematic of LUPI double pass configuration.

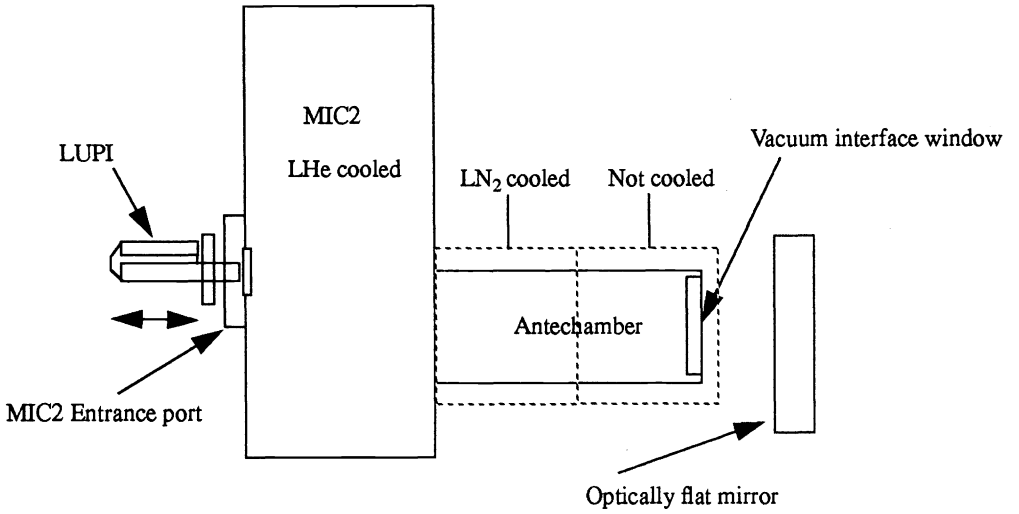

Figure 3. Double pass interferometric MIC2 image quality experiment.

To quantify an adjustment that places the aperture at the optimum focus of the collimator, it is necessary to refer interferometric measurements to the position of the aperture. A classical knife edge test[6] was used to determine this reference point. The test aligns the beam diverger focus with the opening of the aperture, which is located near the focal point of the collimator, and identifies this position. Figure 4 shows a schematic of the knife edge test. In this figure, the beam diverger focus is misaligned with the opening of the aperture. During the test, when the beam diverger focus was inside the aperture, a shadow appeared at the bottom of the CCD display. When the focus was on the outside, the shadow appeared at the top. When the edge of the aperture was aligned with the diverger focus, the CCD display darkened suddenly with small translations. The uncertainty of the aligned position provides an estimate of the fundamental limit at which the best focus can be determined. The uncertainty of the interferometer position using the knife edge test was estimated to be 0.013 inches.

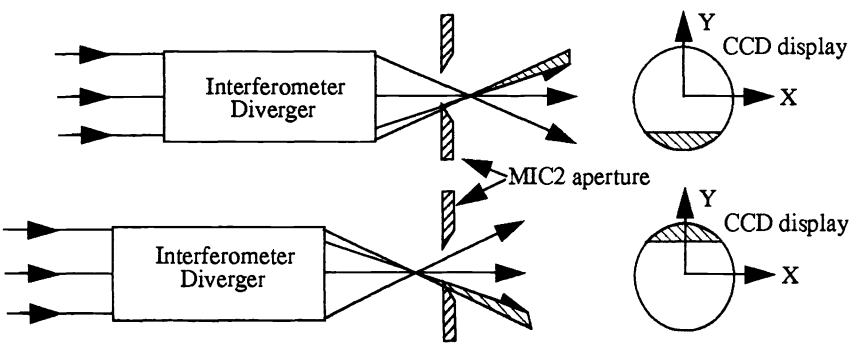

Figure 4. Knife edge test to identify interferometer focus relative to the opening of MIC2's aperture.

3.2 Wavefront Characterization of MIC2

Five interferograms were obtained at two different focus positions near optimal focus to improve the estimate of the wavefront and to characterize the repeatability of this measurement. An estimate of optimal focus was made during image quality testing by observing the interferometer position where the least number of fringes appeared on the interferogram. Fringe tracing of the measured interferograms were performed by digitizing the fringe valleys and assigning a fringe order. This was accomplished using FAST! V/AI[7] software, an enlarged picture of the measured interferogram, and a digitization pad. Tilt was purposely added to the interferogram to aid in the digitization process. An interferogram with added tilt creates a larger set of fringe centers and provides near uniform sampling. Figure 5 shows two measured interferograms, with and without added tilt. The border of the interferogram defines MIC2's exit pupil. The "mouse" bite in the upper right hand corner of the interferogram is from internal baffling that was added to block light from a degraded portion of the optics. The size of MIC2's exit pupil was verified by blocking the reference beam and placing a known grid pattern (1 grid square = 0.563 inches) into the collimated beam during interferometric testing, as shown in Figure 6.

Tilt in the interferogram also reduces fringe ordering ambiguity. This can be seen by comparing the interferograms in Figure 5. The null interferogram contains unbroken fringes on the left and right side of the exit pupil that represent the same OPD. Therefore, the same fringe order must be assigned and detailed analysis must be performed to ensure proper ordering. The interferogram with added tilt, however, contains more uniformly sampled fringes and fringes may be ordered from left to right without ambiguity.

The sign of the wavefront is not contained in a single interferogram and the arbitrary assignment of the fringe order determines the sign of the characterized wavefront. Because the primary aberration in MIC2 optics is astigmatism, sign was determined by identifying the sagittal and tangential focus during interferometric image quality testing. By relating the interferometer longitudinal position for each of the foci, it was possible to identify the sign of the wavefront.

The system wavefront was characterized by fitting the digitized interferogram with Zernike polynomials[6, 7] using the FAST! V/AI software. Figure 7 shows an example of the characterized wavefront for MIC2 expressed in waves where $\lambda = 1.3$ μm. The coefficients were scaled to $\lambda = 12$ μm and stored for later use.

NULL

WITH ADDED TILT

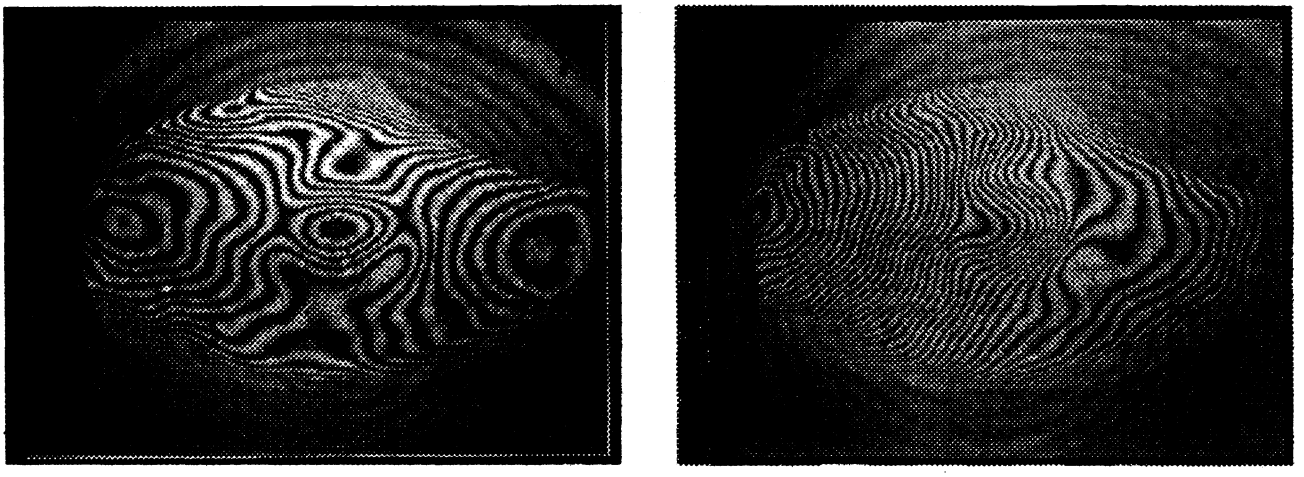

Figure 5. Measured MIC2 interferograms.

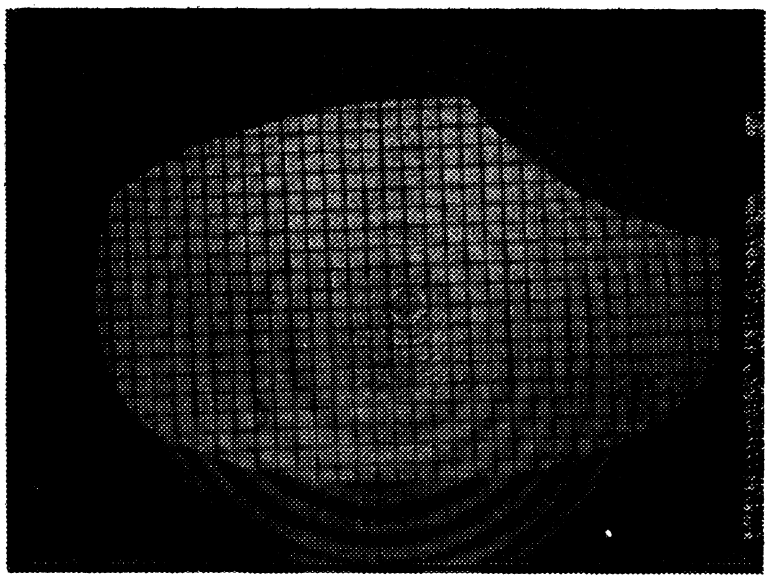

Figure 6. MIC2 exit pupil with superimposed grid pattern.

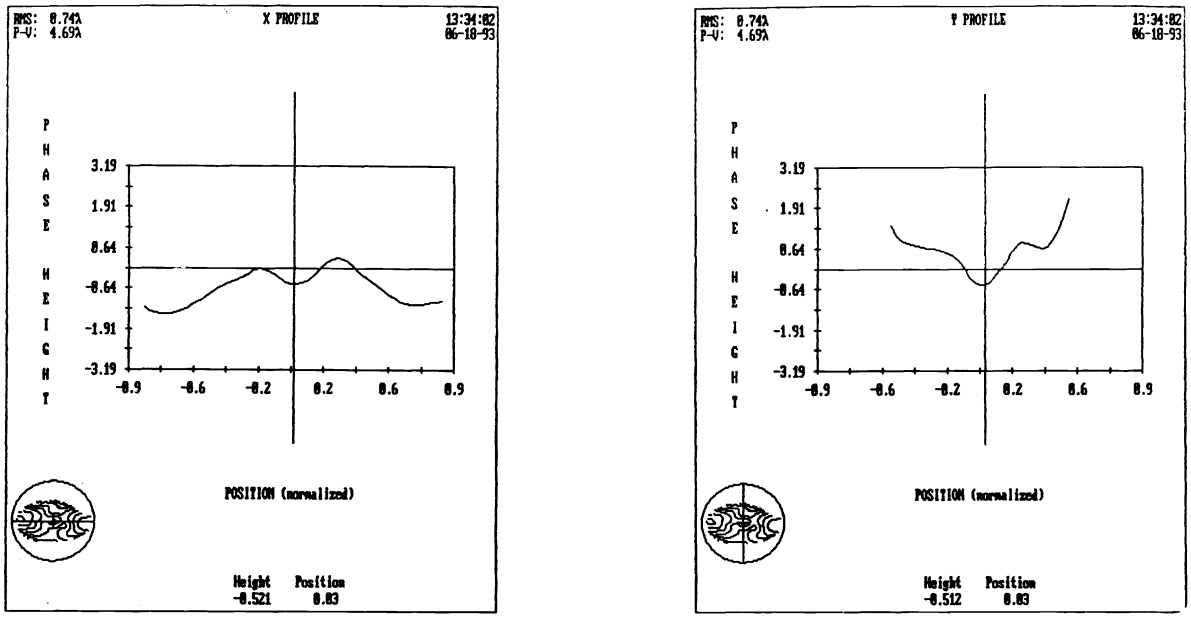

Figure 7. Plot of characterized wavefront using Zernike polynomials.

3.3 Optical Modeling

A qualitative estimate of the optimal focus was made from the LUPI image quality measurements by identifying the focus at which the interferogram contains the least number of fringes. The ability to visually distinguish fluffed out fringes depends on the relative magnitude of image quality, wavelength of measurement, and the system focal length. If a system contains aberrations where it is difficult to visually identify fluffed out fringes over an acceptable range of focus uncertainty, quantitative analysis must be performed to identify optimal focus. We quantified the optimum focus of MIC2 by generating an optical model and adding the characterized wavefront error to simulate the system aberrations.

To quantify the optimum focus relative to the position of the aperture, we applied system level interferometric measurements to an aberration-free optical model of MIC2. We used OSLO optical design software[8] as the optical analysis platform. The Zernike coefficients of the characterized wavefront error for $\lambda = 12$ μm were added to the model's exit pupil by using the Zernike surface option in OSLO. Because the definition of the Zernike coefficients for FAST! V/AI differs from that of OSLO, a transformation had to be performed before the coefficients were entered. The MIC2 model was then coupled to a model of a perfect re-imaging system with the same entrance pupil as the intended application. This was important for our application because the entrance pupil of the re-imaging system (i.e., sensor to be calibrated) is over-filled in one axis and under-filled in the other by MIC2's exit pupil. Figure 8 shows the relationship of the MIC2 model and ideal re-imaging system.

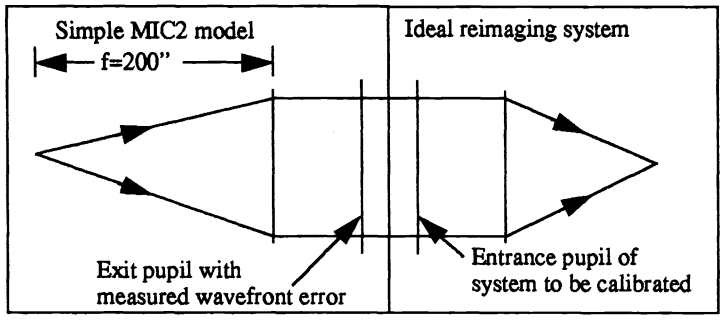

Figure 8. Ray trace schematic of MIC2 and ideal reimaging system.

The pin hole source for the MIC2 model was translated ± 0.4 inches with an increment of 0.0125 inches along the system optical axis to simulate defocus. Figure 9 shows model results of the point spread function for defocus values of -0.4, 0.0, and +0.4 inches. The optimal focus is shown with Δf = 0.0 inches, where the point spread function is smallest and symmetrical. The astigmatism of the system is seen by observing the sagittal or tangential elongation of the point spread function for the defocused results.

Three image quality figures of merit were calculated from the model results at each focus. They were RMS wavefront error, peak-to-valley wavefront error, and 90 μrad encircled energy. All of these figures are related to each other, but are not necessarily optimized at the same focus position. This is especially true when the system is geometrically limited at the wavelength of interest. However, as the system approaches and enters the diffraction limit at longer wavelengths, optimizing the figures of merit results in approximately the same focus.

4. RESULTS

Figure 10 shows the results for the five measured interferograms collected during image quality testing of MIC2 prior to optimizing focus. On these graphs, the position of the aperture is located at 0.00 inches, and the position of optimum focus is shown by the vertical bar. We used the 90 μrad encircled energy and minimum RMS wavefront error to identify optimum focus. The 90 μrad encircled energy was chosen because it matches the spatial resolution of the IR sensor that was to be calibrated. The RMS wavefront error was used because it describes the overall flatness of the wavefront. The peak-to-valley wavefront error did not provide a good measure of the wavefront's overall flatness and was therefore not used. Figure 10 shows the position of optimum focus to be 0.150 inches inside the position of the aperture. The tolerable focus shift, if MIC2 were diffraction limited at λ = 12 μm, is also approximately 0.15 inches, as shown by Equation (2). This provides a comparison of the diffraction limit to the amount of defocus that occurs when MIC2's optics are cooled to cryogenic temperatures. However, image quality may be improved by positioning the aperture at optimum focus because MIC2 optics are not entirely diffraction limited.

The MIC2 aperture was adjusted based on the direction and magnitude of the results shown in Figure 10. Image quality interferometric testing and optical analysis were repeated after focus refinement to verify the new focus. These results are shown in Figure 11 and indicate that the MIC2 aperture was located at the optimum focus. Hence, the focus of MIC2 was successfully optimized.

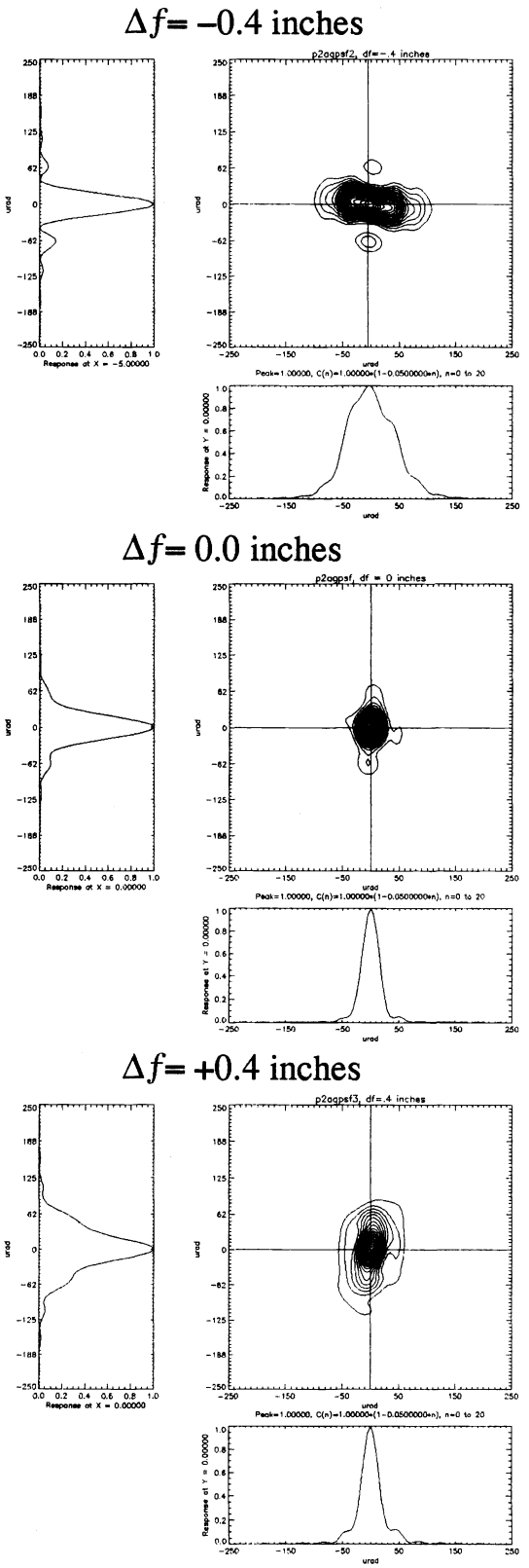

Figure 9. Point spread function model results for three positions of focus.

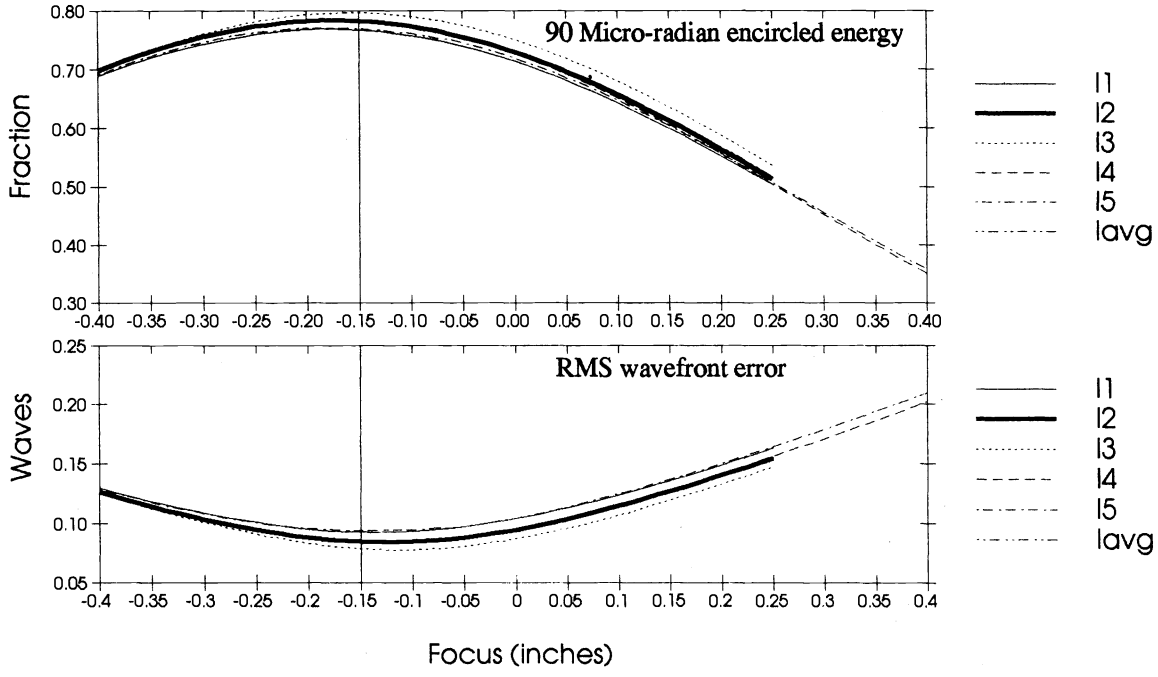

Figure 10. MIC2 pre-focus adjustment (λ = 12 μm).

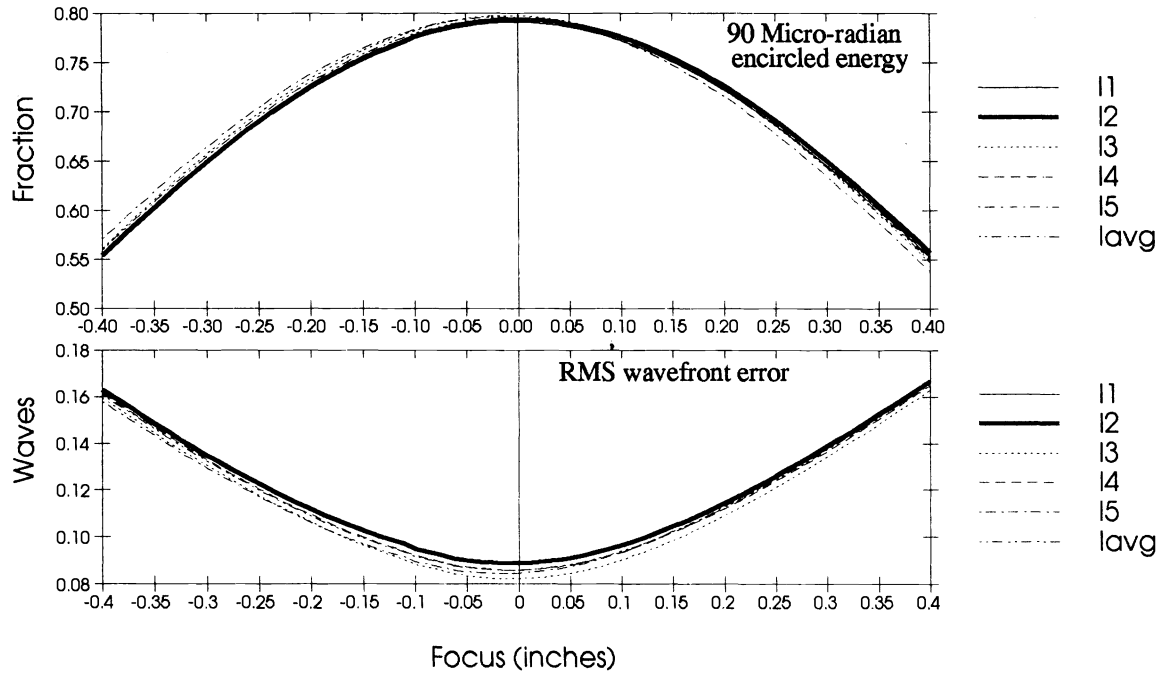

Figure 11. MIC2 post-focus adjustment (λ = 12 μm).

5. SUMMARY

Because of the need to pump and cool cryogenic systems, they typically require long time periods between cold tests and time constraints usually prohibit successive iterations to refine focus. SDL quantified and optimized the focus of a multifunction infrared calibration source (MIC2) for cryogenic operating temperatures. Detailed interferometric image quality testing was performed to characterize the system wavefront error. The characterized wavefront was scaled to $\lambda = 12$ μm and applied to an aberration-free optical model of MIC2. The model was then used to identify optimum focus for the intended application. After an implemented focus refinement based on the results of the optical model, image quality testing and analysis were repeated to verify the new focus. These results confirm the ability to quantify and optimize focus of a cryogenic collimator without iterative cold tests.

REFERENCES

1. W. J. Smith, "Modern Optical Engineering, The Design of Optical Systems," McGraw-Hill, 1966.

2. M. Born and E. Wolf, "Principles of Optics, Electromagnetic Theory of Propagation, Interference And Diffraction of Light," 3rd Edition, Pergamon Press.

3. G. W. Willey and R. J. Patchin, "Optical design analysis incorporating actual system interferometric data," Optical Engineering, Vol. 32 No. 2, pp. 401-409, Feb. 1993.

4. C. L. Wyatt, L. Jacobsen, and A. Steed, "Portable compact multifunction IR calibrator," Proceedings of SPIE - The International Society of Optical Engineering, Vol. 940, pp. 63-72, 1988.

5. Buccini Instrument Company, "MIC-1 Users Guide," 33 Washington Street, Bedford, MA 01730.

6. Daniel Malacara, ed., "Optical Shop Testing," Wiley Series in Pure and Applied Optics, second edition, John Wiley and Sons, Inc., 1992.

7. FAST! V/AI Operations Manual, Phase Shift Technology, Inc. 2601 North Campbell Avenue, Suite 101, Tucson, Arizona 85719, April 1990.

8. OSLO Series 2 and 3 Operating Manual, Sinclair Optics, Inc., 6780 Palmyra Rd. Fairport, NY 14450, 1991.

ACKNOWLEDGEMENTS

The authors wish to acknowledge the valuable contributions of Andrew Shumway, Steve Dansie, Steve Sargent, and Peg Cashell. Their technical input and hard work made this effort possible.